H∞/LPV controller design for an active anti-roll bar system of heavy vehicles using parameter dependent weighting functions

van Tan Vu, Olivier Sename, Luc Dugard, Peter Gáspár

LPV control design by using LPVTools^{TM} for an active anti-roll bar system of heavy vehicles

Van Tan Vu[a,c,*], Olivier Sename[a], Luc Dugard[a], Peter Gaspar[b]

[a] *Univ. Grenoble Alpes, CNRS, GIPSA-lab, Control Systems Department, Grenoble, France*
[b] *Systems and Control Laboratory, Institute for Computer Science and Control, Hungarian Academy of Sciences, Budapest, Hungary*
[c] *Department of Automotive Mechanical Engineering, University of Transport and Communications, Hanoi, Vietnam*

Abstract

Vehicle rollover is a very serious problem for the safety of heavy vehicles, which can result in large financial and environmental consequences. In order to enhance the roll stability, most modern heavy vehicles are equipped with passive anti-roll bars. However they may be not sufficient to overcome critical situations, e.g during cornering or riding on uneven roads, at high speed. This paper is concerned with active anti-roll bar H_∞/LPV control for single unit heavy vehicles. A Linear Parameter Varying (LPV) approach is proposed here in order to schedule the controller with the vehicle forward velocity (that is the varying parameter of the vehicle LPV model) and with the normalized load transfers at the two axles (that are considered into parameter dependent weighting functions for on-line performance adaptation to the rollover risk of heavy vehicles). The grid-based LPV approach is here used to synthesize the H_∞/LPV controller through LPVTools^{TM}. The effectiveness of the H_∞/LPV active anti-roll bar control is validated by using the TruckSim$^{®}$ simulation software with two different types of heavy vehicle: a bus and a truck, both fully loaded. The simulation results in the frequency and time domains show that the H_∞/LPV active anti-roll bar control drastically improves the roll stability of the single unit heavy vehicle compared with the passive anti-roll bar case.

Keywords: Vehicle dynamics, Active anti-roll bar system, Linear Parameter Varying *(LPV)* control, H_∞ control, Roll stability

1. Introduction

1.1. Background

Rollover of heavy vehicles is an important road safety problem world-wide. Although rollovers are relatively rare events, they are usually deadly accidents when they occur. According to the Federal National Highway Traffic Safety Administration (NHTSA), in the United States, there were 333,000 heavy vehicles involved in traffic crashes during 2012. There were 3,921 people killed in rollover crashes and 104,000 people injured (an increase of 18 percent from 2011). Rollover accidents are classified into four categories: preventable, potentially preventable, non-preventable and preventable unknown [1]. It is usually difficult for the driver to feel the rollover behaviour of a heavy vehicle. Investigations have shown that only a minority of rollover accidents could have been avoided with a warning device, potentially more with a skilled driver, but half of the rollover accidents were not preventable by driver action alone. The three major contributing factors to rollover accidents are side wind gusts, abrupt steering and braking manoeuvres by the driver. The main reason of rollover accidents in which heavy vehicles are involved is the roll stability loss when the tyre-road contact force on one of the side wheels becomes zero.

In order to prevent the rollover of vehicles, several schemes concerned with the possible active intervention onto the vehicle dynamics have been proposed as follows: active steering [2], active braking [3], active suspension [4], [5] and active anti-roll bars [6]. Among them, the active anti-roll bar system is the most common method used to improve the roll stability of heavy vehicles.

Active anti-roll bars are usually made of a pair of hydraulic actuators. Lateral acceleration makes vehicles with conventional passive suspension tilt out of corners. The center of the sprung mass shifts outward of the ve-

*Corresponding author. Tel. +33 4 76 82 63 28
Email address:
Van-Tan.Vu@gipsa-lab.grenoble-inp.fr (Van Tan Vu)

hicle centerline, which creates a destabilizing moment that degrades roll stability. The lateral load response is reduced by active anti-roll bars that generate a stabilizing moment to counterbalance the overturning moment in such a way that the control torque leans the vehicle into the corners [7], [8]. One drawback of active anti-roll bars is that the maximum stabilizing moment is limited physically by the relative roll angle between the body and the axle [9].

Linear Parameter Varying (LPV) systems are an important class of systems, whose dynamics depend linearly on the state and input of the system, but could depend in a nonlinear way on scheduling parameters. The LPV paradigm considers that no a priori information about the scheduling parameter values is available, but that the parameter can be measured or estimated online [10], [11].

The interest in LPV systems is motivated by their use in gain-scheduling control techniques, and by the possibility to embed nonlinear systems into the LPV framework by covering nonlinearities within the scheduling parameters. Therefore the LPV framework enables, to some extent, the application of linear control methods to nonlinear systems, while providing rigorous statements on stability and performance of the closed-loop system.

1.2. Related works

In the literature, many works have been dedicated to design the active anti-roll bar system for single unit heavy vehicles.

Many control strategies have been developed using the **yaw-roll model** such as:

- **Optimal control:** In [9], [12], [13] the authors used *LQR* method for the active anti-roll bar system of heavy vehicles. The control torques acting between the axle groups and the sprung mass are considered as the input control signal. The simulation results indicated that the normalized load transfers at all the axles reduced significantly, compared with the passive anti-roll bar system at 60 km/h.

- H_∞ **and LPV control:** In [7], [14], [15] the LPV approach is applied for the active anti-roll bar system combined with active brake control on a single unit heavy vehicle. The forward velocity was considered as the varying parameter. The different actuator failures are identified by using a Fault Detection and Identification *(FDI)* filter.

  The H_∞ control method was also applied to the yaw-roll model of a single unit heavy vehicle. It shows, using μ tool analysis, that the H_∞ active anti-roll bar control is robust w.r.t. the forward velocity and sprung mass variations [16].

TruckSim® software is also used to evaluate the effectiveness of the active roll control system of heavy vehicles [17]. The simulations performed using TruckSim® indicated that a rollover threat detection system was further enhanced in combination with an active roll control system using active suspension mechanism.

In [18], [19] the authors proposed an **integrated model** with four electronic servo-valve hydraulic actuator models in a single unit heavy vehicle yaw-roll model. Then the *LQR* control method was applied to the active anti-roll bar, showing how it may solve a multi-objective problem considering the improvement of the roll stability, while taking into account the characteristics of the electronic servo-valve hydraulic actuators.

1.3. Paper contribution

Based on the integrated model presented in [19], this paper proposes a MIMO H_∞/LPV controller, with three varying parameters (forward velocity and normalized load transfers at the two axles), designed using the grid-based LPV approach [20]. Hence, the main contributions of this paper can be summarized in the following points:

- Parameter dependant weighting functions are used to allow for performance adaptation to the rollover risk of heavy vehicles, characterized by the normalized load transfers at the two axles.
- The grid-based LPV approach [20] is used to synthesize the H_∞/LPV controller depending on three varying parameters, which are the forward velocity and the normalized load transfers at the two axles. It is the first time that the grid-based LPV approach is applied for the heavy vehicle dynamic through LPVTools™.
- The H_∞/LPV active anti-roll bar control is validated using the TruckSim® simulation software with two different types of vehicle: a tour bus and a LCF (Low Cab Forward) truck, both fully loaded.
- The simulation results, in the frequency and time domains, show that the H_∞/LPV active anti-roll bar control is a realistic solution which drastically improves the roll stability of a single unit heavy vehicle compared with the passive anti-roll bar.

This paper is organised as follows: Section 2 details the LPV model of a single unit heavy vehicle with the forward velocity as scheduling parameter. Section 3 proposes the formulation of the H_∞/LPV control problem. Section 4 illustrates the solution of the H_∞/LPV control

problem. Section 5 gives the simulation results analysis in the frequency and time domains where the LPV active anti-roll bar controller is compared with the passive anti-roll bar case. Validation of the H_∞/LPV active anti-roll bar control by using the TruckSim® simulation software is analysed in section 6. Finally, some conclusions are drawn in section 7.

2. Vehicle modelling: an LPV approach

The integrated model of a single unit heavy vehicles was proposed in [19]. It includes four Electronic Servo-Valve Hydraulic (ESVH) actuators (two at the front and two at the rear axles) mounted in a linear yaw-roll model. In each ESVH actuator, the control signal is the electrical current u opening the electronic servo-valve, the output is the force F_{act} generated by the hydraulic cylinder.

2.1. The electronic servo-valve hydraulic actuator model [19]

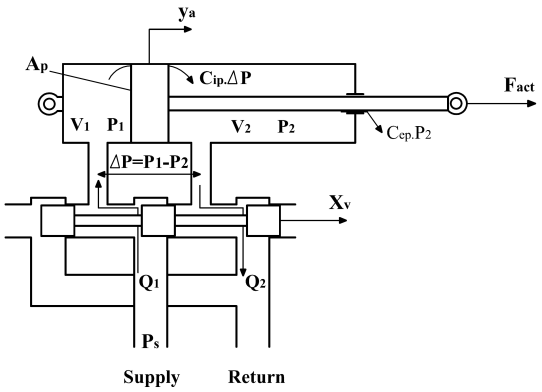

Figure 1: Diagram of the ESVH actuator [21].

Figure 1 illustrates the diagram of the considered ESVH actuator, made of an electronic servo-valve and a hydraulic cylinder. The spool valve displacement X_v of the electronic servo-valve is controlled by the current u. The oil supply high pressure P_s is always stored outside the electronic servo-valve and the spool valve displacement distributes high pressure oil into the two chambers of the hydraulic cylinder. The difference of pressures $\Delta P = P_1 - P_2$ inside the two chambers produces the output force F_{act}. The dynamical equations of the ESVH actuator are presented in equation (1) and the symbols are shown in Table 1.

$$\begin{cases} F_{act} = A_P \Delta P \\ \frac{V_t}{4\beta_e}\frac{d\Delta P}{dt} + (K_P + C_{tp})\Delta P - K_x X_v + A_P \frac{dy_a}{dt} = 0 \\ \frac{dX_v}{dt} + \frac{1}{\tau}X_v - \frac{K_v}{\tau}u = 0 \end{cases} \quad (1)$$

where y_a is the displacement of the piston inside the hydraulic cylinder, u the input current to the servo-valve.

Table 1: Symbols of the ESVH actuator [1], [22].

Symbols	Description
A_P	Area of the piston
K_x	Valve flow gain coefficient
K_P	Total flow pressure coefficient
C_{tp}	Total leakage coefficient of the actuator
V_t	Total volume of trapped oil
β_e	Effective bulk modulus of the oil
τ	Time constant of the servo-valve
K_v	Servo-valve gain

2.2. Yaw-roll model of a single unit heavy vehicle [14]

The linear yaw-roll model is shown in the Figure 2, the differential equations of motion, i.e., the lateral dynamics, the yaw moment, the roll moment of the sprung mass, the roll moment of the unsprung masses at the two axles, are formalized in the equations (2):

$$\begin{cases} mv(\dot\beta + \dot\psi) - m_s h\ddot\phi = F_{yf} + F_{yr} \\ -I_{xz}\ddot\phi + I_{zz}\ddot\psi = F_{yf}l_f - F_{yr}l_r \\ (I_{xx} + m_s h^2)\ddot\phi - I_{xz}\ddot\psi = m_s v h(\dot\beta + \dot\psi) \\ \quad + m_s g h\phi - k_f(\phi - \phi_{uf}) - b_f(\dot\phi - \dot\phi_{uf}) \\ \quad + T_f - k_r(\phi - \phi_{ur}) - b_r(\dot\phi - \dot\phi_{ur}) + T_r \\ -rF_{yf} = m_{uf} v(r - h_{uf})(\dot\beta + \dot\psi) \\ \quad + m_{uf} g h_{uf}.\phi_{uf} - k_{tf}\phi_{uf} \\ \quad + k_f(\phi - \phi_{uf}) + b_f(\dot\phi - \dot\phi_{uf}) + T_f \\ -rF_{yr} = m_{ur} v(r - h_{ur})(\dot\beta + \dot\psi) - m_{ur} g h_{ur}\phi_{ur} \\ \quad - k_{tr}\phi_{ur} + k_r(\phi - \phi_{ur}) + b_r(\dot\phi - \dot\phi_{ur}) + T_r \end{cases} \quad (2)$$

where T_f and T_r are the torques generated by the active anti-roll bar system at the front and rear axles. The lateral tyre forces $F_{yf,r}$ in the direction of velocity at the wheel ground contact points are modelled by a linear stiffness as:

$$\begin{cases} F_{yf} = \mu C_f \alpha_f \\ F_{yr} = \mu C_r \alpha_r \end{cases} \quad (3)$$

with tyre side slip angles:

$$\begin{cases} \alpha_f = -\beta + \delta_f - \frac{l_f \dot\psi}{v} \\ \alpha_r = -\beta + \frac{l_r \dot\psi}{v} \end{cases} \quad (4)$$

The symbols of the yaw-roll model of a single unit heavy vehicle are detailed in Table 2.

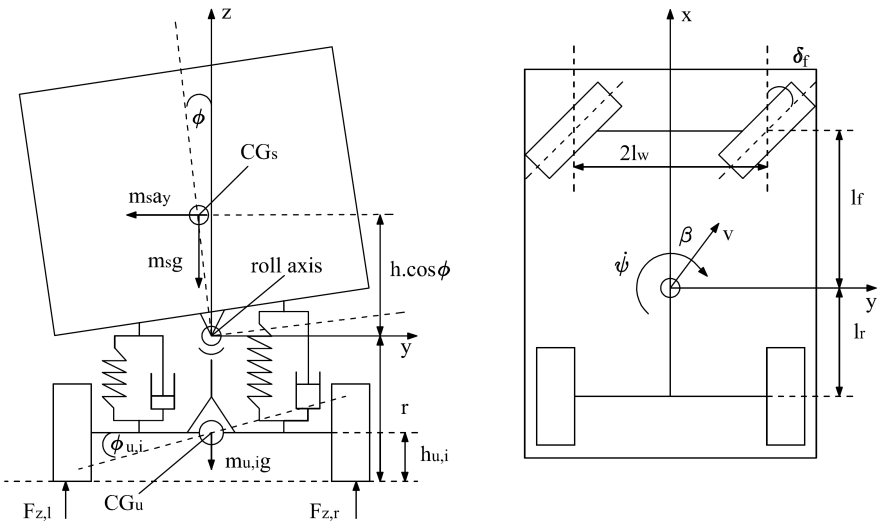

Figure 2: Yaw-Roll model of a single unit heavy vehicle [14].

The forces, as well as other characteristics of the ESVH actuators at each axle, do have the same magnitude and the opposite direction [19], therefore we can consider that the torque generated by the active anti-roll bar system at each axle is twice the torque generated by one electronic servo-valve hydraulic actuator. In this study, the characteristics of the ESVH actuators on the right at the front, and on the right at the rear axles will be used. The torque generated by the active anti-roll bar system at the front axle is determined by:

$$T_f = 2l_{act}F_{actf} = 2l_{act}A_p\Delta_{Pf} \tag{5}$$

and the torque generated by the active anti-roll bar system at the rear axle is:

$$T_r = 2l_{act}F_{actr} = 2l_{act}A_p\Delta_{Pr} \tag{6}$$

where Δ_{Pf} and Δ_{Pr} are respectively the difference of pressure of the hydraulic cylinder at the front and rear axles.
The dynamical equations (1) of the ESVH actuators are written in the integrated model of a single unit heavy vehicle as follows:

$$\begin{cases} \frac{V_t}{4\beta_e}\dot{\Delta}_{Pf} + (K_P + C_{tp})\Delta_{Pf} - K_x X_{vf} \\ \quad + A_p l_{act}\dot{\phi} - A_p l_{act}\dot{\phi}_{uf} = 0 \\ \dot{X}_{vf} + \frac{1}{\tau}X_{vf} - \frac{K_v}{\tau}u_f = 0 \\ \frac{V_t}{4\beta_e}\dot{\Delta}_{Pr} + (K_P + C_{tp})\Delta_{Pr} - K_x X_{vf} \\ \quad + A_p l_{act}\dot{\phi} - A_p l_{act}\dot{\phi}_{ur} = 0 \\ \dot{X}_{vr} + \frac{1}{\tau}X_{vr} - \frac{K_v}{\tau}u_r = 0 \end{cases} \tag{7}$$

The combination of equations (2) to (7) are the motion differential equations of the integrated model of a single unit heavy vehicle.

2.3. An LPV model of a single unit heavy vehicle

We can see in (2)-(4) that the yaw-roll model depends on the forward velocity v and on the inverse of the forward velocity $\frac{1}{v}$. Moreover, when the vehicle is in motion, the forward velocity is one of the constantly changing parameters, and it depends on the driver and the motion condition of the vehicle. Here, the forward velocity v is chosen as a scheduling parameter.
Denoting $\rho_1 = v$, the integrated model of a single unit heavy vehicle, merging the equations (2)-(7) is written in the state-space representation form as follows:

$$\dot{x} = A(\rho_1).x + B_1(\rho_1).w + B_2(\rho_1).u \tag{8}$$

where ρ_1 is a varying parameter and the state vector:

$$x = \begin{bmatrix} \beta & \dot{\psi} & \phi & \dot{\phi} & \phi_{uf} & \phi_{ur} & \Delta_{Pf} & X_{vf} & \Delta_{Pr} & X_{vr} \end{bmatrix}^T$$

The exogenous disturbance (steering angle) is:

$$w = \begin{bmatrix} \delta_f \end{bmatrix}^T$$

and the control inputs (input currents):

$$u = \begin{bmatrix} u_f & u_r \end{bmatrix}^T$$

The model (8) is transformed into a Linear Parameter Varying (LPV) model, whose state-space entries depend continuously on a time varying parameter vector,

$\rho_1(t)$. One characteristic of the LPV system is that it must be linear in the pair formed by the state vector (x), and the control input vector (u). The matrices $A(\rho_1)$, $B_1(\rho_1)$ and $B_2(\rho_1)$ are generally nonlinear functions of the scheduling vector ρ_1.

Remark: Let us note that $A(\rho_1)$ is not affine in ρ_1 since it includes ρ_1 and $\frac{1}{\rho_1}$. Therefore the classical polytopic approach cannot be used unless we consider two different parameters, which increases the conservatism.

Table 2: Symbols of the yaw-roll model.

Symbols	Description
m_s	Sprung mass
$m_{uf,r}$	Unsprung masses
m	The total vehicle mass
v	Forward velocity
h	Height of sprung mass from roll axis
$h_{uf,r}$	Height of unsprung mass from ground
r	Height of roll axis from ground
a_y	Lateral acceleration
β	Side-slip angle at center of mass
ψ	Heading angle
$\dot{\psi}$	Yaw rate
α	Side slip angle
ϕ	Sprung mass roll angle
$\phi_{uf,r}$	Roll angle of unsprung masses
δ_f	Steering angle
$u_{f,r}$	Control currents
$C_{f,r}$	Tyre cornering stiffness on the axles
$k_{f,r}$	Suspension roll stiffness on the axles
$b_{f,r}$	Suspension roll damping on the axles
$k_{tf,r}$	Tyre roll stiffness on the axles
I_{xx}	Roll moment of inertia of sprung mass
I_{xz}	Yaw-roll inertial of sprung mass
I_{zz}	Yaw moment of inertia of sprung mass
$l_{f,r}$	Length from the CG to the axles
l_w	Half of the vehicle width
μ	Road adhesion coefficient

3. Formulation of the H_∞/LPV control problem

3.1. Performance criteria

To evaluate the rollover of vehicles, let us first consider the tyre force (F_z) in the Z direction at the each wheel. The rollover occurs when $F_z = 0$, and the wheel then starts to lift off the road.

However the value of the tyre force (F_z) in the Z direction at the each wheel is not easy to measure or estimate. For the yaw-roll model of the heavy vehicles in Figure 2, the normalized load transfer $R_{f,r}$ (9) at the two axles is also used to evaluate the rollover, defined in [7], [17], [23]. When the value of $R_{f,r}$ takes on the limit of ± 1, the wheel in the inner bend lifts off the road, and the rollover occurs.

$$R_f = \frac{\Delta F_{zf}}{F_{zaf}}, \quad R_r = \frac{\Delta F_{zr}}{F_{zar}} \tag{9}$$

where F_{zaf} is the total axle load at the front axle and F_{zar} at the rear axle. ΔF_{zf} and ΔF_{zr} are respectively the lateral load transfers at the front and rear axles, which can be given by:

$$\Delta F_{zf} = \frac{k_{uf}\phi_{uf}}{l_w}, \quad \Delta F_{zr} = \frac{k_{ur}\phi_{ur}}{l_w} \tag{10}$$

In the case of an obstacle avoidance in an emergency, the wheels at the rear axle lift off first for the truck, because the rollover of a vehicle is affected by the suspension stiffness to load ratio, which is greater at the rear axle than at the front one [6], [7]. However the other effect to be considered in the rollover of a vehicle is the distribution of the total load for the two axles. In the case of big buses, the engine is often mounted at the rear, so the wheels at the front axle usually lift off first. Therefore generally it is necessary to consider the rollover risk at the two axles of heavy vehicles.

Since such performance indices are key parameters to evaluate the risk of rollover, they are considered here as scheduling parameters of the LPV control, in order to provide a stable and smooth control action when reaching critical situations. Let us note that a similar idea was used in [7], [14] considering the rear load transfer only in order to account for actuator fault and to switch on braking actuations when critical situations occur.

We then define $\rho_2 = |R_f|$ and $\rho_3 = |R_r|$.

3.2. Performance specifications for the H_∞/LPV control design

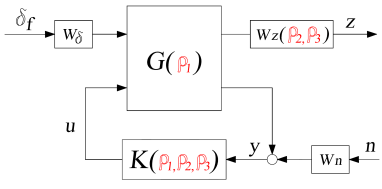

Figure 3: The closed-loop interconnection structure of the LPV active anti-roll bar control.

In this section the LPV control problem is presented for the active anti-roll bar system of heavy vehicles, using ESVH actuators. In Figure 3, the given H_∞/LPV

control structure includes the nominal model $G(\rho_1)$, the controller $K(\rho_1,\rho_2,\rho_3)$, the performance output z, the control input u, the measured output y, the measurement noise n. The steering angle δ_f is the disturbance signal, set by the driver. The weighting functions $W_\delta, W_z(\rho_{2,3}), W_n$ are presented thereafter, according to the considered performance objectives.

The weighting functions matrix W_z representing the performance output, is chosen as $W_z = diag[W_{zu}, W_{zR}]$. The purpose of the weighting functions is to keep the control inputs and normalized load transfers as small as possible over the desired frequency range up to $4 rad/s$, which represents the limited bandwidth of the driver [7], [9]. These weighting functions can be considered as penalty functions, that is, weights which should be large in the frequency range where small signals are desired and small where larger performance outputs can be tolerated.

The weighting function W_{zu} is chosen as $W_{zu} = diag[W_{zuf}, W_{zur}]$, corresponding to the input currents at the front and rear axles. The reason for keeping the control signals small is to avoid the actuator saturation, and they are selected as:

$$W_{zuf} = \frac{1}{0.4}; \quad W_{zur} = \frac{1}{0.4} \tag{11}$$

The weighting function W_{zR}, chosen as $W_{zR} = diag[W_{zRf}, W_{zRr}]$, corresponds to the normalized load transfers at front and rear axles, and is selected as:

$$W_{zRf} = \rho_2 \frac{\frac{s}{20}+1}{\frac{s}{100}+15}; \quad W_{zRr} = \rho_3 \frac{\frac{s}{20}+1}{\frac{s}{100}+15} \tag{12}$$

The authors stress that the interest of parameter dependant weighting functions is to allow for performance adaptation to the rollover risk of heavy vehicles. Indeed, the ESVH actuators will be tuned according to the varying parameters in order to meet the desired performance. For example, as far as the normalized load transfer at the front is concerned, when the varying parameter $\rho_2 \to 1$, the gain of the weighting function W_{zRf} is large, and therefore the normalized load transfer at the front will be penalized. In the same way, when ρ_3 is large, the normalized load transfer at the rear will be reduced.

The input scaling weight W_δ normalizes the steering angle to the maximum expected command. It is selected as $W_\delta = \pi/180$, which corresponds to a 1^0 steering angle command.

The weighting function W_n is selected as a diagonal matrix which accounts for sensor noise models in the control design. The noise weights are chosen as $0.01(m/s^2)$ for the lateral acceleration and $0.01(^0/sec)$ for the derivative of the roll angle $\dot{\phi}$ [7].

3.3. The LPV generalized plant

According to Figure 3, the concatenation of the nonlinear model (8) with the performance weighting functions has a partitioned representation in the following way:

$$\begin{bmatrix} \dot{x}(t) \\ z(t) \\ y(t) \end{bmatrix} = \begin{bmatrix} A(\rho) & B_1(\rho) & B_2(\rho) \\ C_1(\rho) & D_{11}(\rho) & D_{12}(\rho) \\ C_2(\rho) & D_{21}(\rho) & D_{22}(\rho) \end{bmatrix} \begin{bmatrix} x(t) \\ w(t) \\ u(t) \end{bmatrix} \tag{13}$$

with the exogenous input $w(t) = \begin{bmatrix} \delta_f & n \end{bmatrix}$, the control input $u(t) = \begin{bmatrix} u_f & u_r \end{bmatrix}^T$, the measured output vector $y(t) = \begin{bmatrix} a_y & \dot{\phi} \end{bmatrix}^T$, and the performance output vector $z(t) = \begin{bmatrix} u_f & u_r & R_f & R_r \end{bmatrix}^T$.

It is worth noting that, in the LPV model of the active anti-roll bar system (13), the varying parameters $\rho = [\rho_1, \rho_2, \rho_3]$ are known in real time. Indeed the parameter $\rho_1 = v$ is measured directly, while the parameters $R_{f,r}$ (ρ_2 and ρ_3) can be calculated by using the measured roll angle of the unsprung masses $\phi_{uf,r}$ [7].

3.4. H_∞/LPV control problem

The control goal is to find a LPV controller $K(\rho)$ defined as:

$$\begin{bmatrix} \dot{x}_K(t) \\ u(t) \end{bmatrix} = \begin{bmatrix} A_K(\rho) & B_K(\rho) \\ C_K(\rho) & D_K(\rho) \end{bmatrix} \begin{bmatrix} x_K(t) \\ y(t) \end{bmatrix} \tag{14}$$

where $A_K(\rho)$, $B_K(\rho)$, $C_K(\rho)$, $D_K(\rho)$ are continuous bounded matrix functions, which minimizes the induced $\mathscr{L}_2$ norm of the closed-loop LPV system $\sum_{CL} = LFT(G,K)$, with zero initial conditions, i.e.:

$$\| \sum_{CL}(\rho) \|_{2\to 2} = \sup_{\substack{\rho\in\mathscr{P} \\ \underline{\nu}\le\dot{\rho}\le\overline{\nu}}} \sup_{\substack{w\in\mathscr{L}_2 \\ \|w\|_2\neq 0}} \frac{\| z(\rho) \|_2}{\| w \|_2} \tag{15}$$

The existence of a controller that solves the parameter dependent LPV γ-performance problem can be expressed as the feasibility of a set of linear matrix inequalities (LMIs), which can be solved numerically [7], [15], [24].

It is worth noting that:

- the above problem can be solved considering the parameter dependent stability of LPV systems, which is the generalization of the quadratic stability concept. Applying the parameter dependent stability concept, it is assumed that the derivative of parameters can also be measured in real time. This concept is less conservative than the quadratic stability [20], [25], [26].

- the possible controller dependence on $\dot{\rho}$ will be stated by the adopted solution in terms of the parameter-dependence, or not, of the Lyapunov matrix.

4. Solution of the H_∞/LPV control problem

Let us consider the LPV generalized plant (13). First, recall that several methods have arisen for representing the parameter dependence in LPV models, and then for designing the LPV controllers, such as [27]:

- **Linear Fractional Transformations (LFT)** [28], [29]: The LFT models have state matrices that are rational functions of the parameter. Hence, their dependence on the parameter vector is modeled explicitly.
- **Polytopic solution**: A polytopic system is a convex combination of systems defined at each vertex of a polytope given by the bounds of the scheduling parameters [30], [31], [32]. The synthesis of such a controller can be made in the framework of H_∞/LPV based on the LMI solution for polytopic systems (the framework of quadratic stabilization). This can be applied to LPV systems with an affine dependence on the parameters only.
- **Linearizations on a gridded domain (grid-based LPV)** [20], [31], which are obtained through Jacobian linearization at each grid point. Each linearization approximates the system's dynamics in the vicinity of a particular grid point, and the grid of linearizations captures the system's parameter dependence implicitly. Hence, linearization based LPV models do not require any special dependence on the parameter vector.

In this research, the authors are interested in the grid-based LPV approach for the active anti-roll bar system of heavy vehicles using the LPVTools^{TM} toolbox [33]. Indeed such an approach is interesting where the number of parameters increases since the polytopic approach may lead to very conservative results (due to the augmented size of the parameter set and the single Lyapunov function). It has been used successfully in several studies [33], [34], [35] and is now available in the LPVTools^{TM} toolbox [36].

4.1. A solution to the LPV control design

Some brief recalls on the synthesis of dynamic and feedback controllers for LPV presented here. More details can be found in the studies [20], [25], [26]. The following theorem describes the LPV analysis problem when it is formulated in terms of the induced $\mathscr{L}_2$ norm of $G(\rho)$ and the rate-bounds $(\bar{\nu}, \underline{\nu})$ of the parameter are taken into account [7].

Theorem 1: Given a compact set $\mathscr{P} \subset \mathscr{R}^S$, the performance level γ and the LPV system (13), with restriction $D_{11}(\rho = 0)$, the parameter-dependent γ-performance problem is solvable if there exist a continuously differentiable function X: $\mathscr{R}^S \to \mathscr{R}^{n\times n}$, and Y: $\mathscr{R}^S \to \mathscr{R}^{n\times n}$, such that for all $\rho \in \mathscr{P}$, $X(\rho) = X^T(\rho) > 0$, $Y(\rho) = Y^T(\rho) > 0$ and

$$\begin{bmatrix} \hat{A}(\rho)X(\rho) + X(\rho)\hat{A}^T(\rho) - \sum_{i=1}^{s}(\nu_i \frac{\partial X}{\partial \rho_i}) - B_2(\rho)B_2^T(\rho) & X(\rho)C_1^T(\rho) & \gamma^{-1}B_1(\rho) \\ C_1(\rho)X(\rho) & -I_{ne} & 0 \\ \gamma^{-1}B_1^T(\rho) & 0 & -I_{nd} \end{bmatrix} < 0, \tag{16}$$

$$\begin{bmatrix} \tilde{A}^T(\rho)Y(\rho) + Y(\rho)\tilde{A}(\rho) + \sum_{i=1}^{s}(\nu_i \frac{\partial Y}{\partial \rho_i}) - C_2^T(\rho)C_2(\rho) & Y(\rho)B_1(\rho) & \gamma^{-1}C_1^T(\rho) \\ B_1^T(\rho)Y(\rho) & -I_{nd} & 0 \\ \gamma^{-1}C_1(\rho) & 0 & -I_{ne} \end{bmatrix} < 0, \tag{17}$$

$$\begin{bmatrix} X(\rho) & \gamma^{-1}I_n \\ \gamma^{-1}I_n & Y(\rho) \end{bmatrix} \geq 0 \tag{18}$$

where $\hat{A}(\rho) = A(\rho) - B_2(\rho)C_1(\rho)$,$\tilde{A}(\rho) = A(\rho) - B_1(\rho)C_2(\rho)$. If the conditions are satisfied, there exists a controller (14) solving that problem. The Theorem 1 and its proof are found in [20], [25], [26].

The constraints set by the LMIs in Theorem 1 are infinite dimensional, as is the solution space. The variables are X, Y: $\mathscr{R}^S \to \mathscr{R}^{n\times n}$, which restricts the search to the span of a collection of known scalar basis functions. Select scalar continuous differentiable basis functions $\{g_i : \mathscr{R}^S \to \mathscr{R}\}_{i=1}^{N_x}$, $\{f_i : \mathscr{R}^S \to \mathscr{R}\}_{j=1}^{N_y}$, then the variables in Theorem 1 can be parametrized as:

$$X(\rho) = \sum_{i=1}^{N_x} g_i(\rho)X_i, \quad Y(\rho) = \sum_{i=1}^{N_y} f_i(\rho)Y_j \tag{19}$$

Currently, there is no analytical method to select the basis functions, namely g_i and f_i. An intuitive rule for the basis function selection is to use those present in the open-loop state space data. In our case, several power series $\{1, \rho^2\}$ of the scheduling parameters are chosen, based on the lowest closed-loop $\mathscr{L}_2$ norm achieved.

4.2. Grid-based LPV approach

The LPV system in the equation (13) is conceptually represented by a state-space system $S(\rho)$ that depends on a time varying parameter vector ρ. A grid-based LPV model of this system is a collection of linearizations on a gridded domain of parameter values [36]. For

general LPV systems, this conceptual representation requires storing the state-space system at an infinite number of points in the domain of ρ. For each grid point $\hat{\rho}_k$ there is a corresponding LTI system $(A(\hat{\rho}_k), B(\hat{\rho}_k), C(\hat{\rho}_k), D(\hat{\rho}_k))$ which describes the dynamics of $S(\hat{\rho}_k)$ when $\hat{\rho}_k$ is held constant. All the linearized systems on the grid have identical inputs u, outputs y and state vectors x. Together they form a LPV system approximation of $S(\rho)$ [35], [37]. Such a grid-based approach is here used to find an LPV controller (14) solving the Theorem 1.

4.3. The LPVTools^{TM} toolbox

LPVTools$^{\text{TM}}$ toolbox was developed by MUSYN, Inc. (G. Balas and the authors) but has been made freely available to the community. The toolbox can is available for download at:
www.aem.umn.edu/ SeilerControl/software.shtml
The LPVTools$^{\text{TM}}$ is a MATLAB toolbox for modeling and design of Linear Parameter-Varying (LPV) systems. The toolbox contains data structures to represent LPV systems in both the LFT and gridded (Jacobian-linearization) framework. The core of the toolbox is a collection of functions for model reduction, analysis, synthesis and simulation of LPV systems. The readers interested in the characteristics and capacities of the LPVTools$^{\text{TM}}$ toolbox, can find more in [33], [36].

4.4. Grid-based LPV approach for the active anti-roll bar system

In this study, the grid-based LPV approach and LPVTools$^{\text{TM}}$ are used to synthesize the H_∞/LPV active anti-roll bar control for heavy vehicles. It requires a gridded parameter space for the three varying parameters $\rho = [\rho_1, \rho_2, \rho_3]$. In the interconnection structure, the spacing of the grid points is selected on the basis of how well the H_∞ point designs perform for plants around the design point. The H_∞ controllers are synthesized for 10 grid points of the forward velocity in the range $\rho_1 = v = [40km/h, 130km/h]$ and 5 grid points of the normalized load transfers at the two axles in a range $\rho_2 = |R_f| = [0,1]$, $\rho_3 = |R_r| = [0,1]$, respectively.
In this work, we have chosen to design a controller that does not depend on the parameter derivatives (so the scalar basis functions (19) are constant). The following commands are used to make the grid points as well as the LPV controller synthesis by using LPVTools$^{\text{TM}}$:
rho1 = pgrid('rho1',linspace(40/3.6,130/3.6,10));
rho2 = pgrid('rho2',linspace(0,1,5));
rho3 = pgrid('rho3',linspace(0,1,5))
and *[Klpv,normlpv] = lpvsyn(H,nmeas,ncont).*
The weighting functions for both the performance and robustness specifications are considered unique for the whole grid. The effect of the proposed H_∞/LPV active anti-roll bar controller to improve the roll stability of heavy vehicles will be proved in the next sections.

5. Simulation results analysis

In this section, the simulation results of the single unit heavy vehicle using the four ESVH actuators with the H_∞/LPV controller are shown both in the frequency and time domains. The parameter values of the ESVH actuators and of the yaw-roll model are those given in Table 3.

Table 3: Parameters of the yaw-roll model and ESVH actuator [7], [18].

Parameter	Value	Parameter	Value
m_s	12487 kg	b_f	100 $\frac{kN}{rad}$
$m_{u,f}$	706 kg	b_r	100 $\frac{kN}{rad}$
$m_{u,r}$	1000 kg	k_{tf}	2060 $\frac{kNm}{rad}$
m	14193 kg	k_{tr}	3337 $\frac{kNm}{rad}$
I_{xx}	24201 kgm^2	k_f	380 $\frac{kNm}{rad}$
I_{xz}	4200 kgm^2	k_r	684 $\frac{kNm}{rad}$
I_{zz}	34917 kgm^2	C_f	582 $\frac{kN}{rad}$
r	0.83 m	C_r	783 $\frac{kN}{rad}$
$h_{u,i}$	0.53 m	l_f	1.95 m
h	1.15 m	l_r	1.54 m
A_P	0.0123 m^2	K_x	2.5 $\frac{m^2}{s}$
K_P	$4.2x10^{-11}$ $\frac{m^5}{Ns}$	C_{tp}	0
β_e	$6.89x10^6$ $\frac{N}{m^2}$	V_t	0.0014 m^3
τ	0.01 s	K_v	0.955 $\frac{in}{A}$

5.1. Analysis in the frequency domain

Various closed-loop transfer functions of the LPV active anti-roll bar system on heavy vehicles are shown in this section. The main objective of the active anti-roll bar system is to reduce the normalized load transfer at each axle $(R_{f,r})$. To evaluate the effectiveness of the proposed H_∞/LPV active anti-roll bar controller, the two following cases will be considered: in the 1^{st} case, the varying parameters are $\rho_1 = v = [40km/h, 130km/h]$, $\rho_{2,3} = 0.5$ and in the 2^{nd} case, the varying parameters are $\rho_{2,3} = [0,1]$, $\rho_1 = v = 70\ km/h$.

5.1.1. The 1^{st} case: $\rho_1 = v = [40km/h, 130km/h]$ (10 grid points)

We only consider the varying parameter $\rho_1 = v = [40km/h, 130km/h]$ with 10 grid points, while the varying parameters $\rho_{2,3}$ are kept constant at 0.5. Figures 4

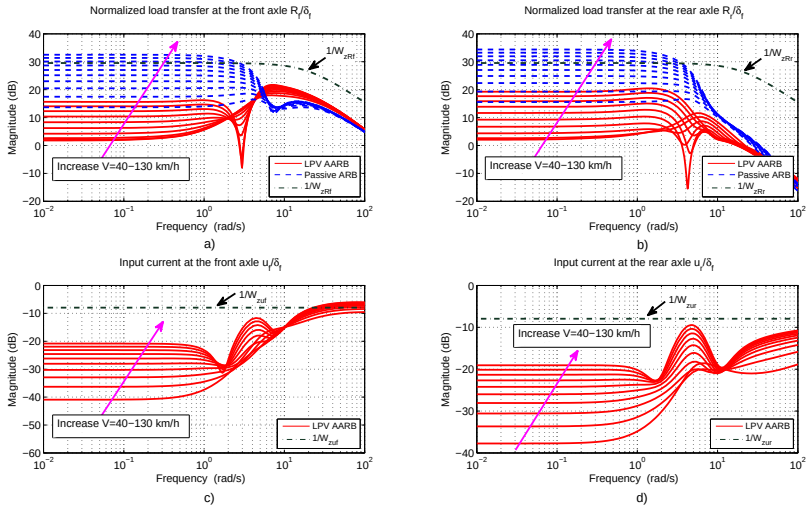

Figure 4: Transfer function magnitude of (a, b) the normalized load transfers $\frac{R_{f,r}}{\delta_f}$, (c, d) the input currents $\frac{u_{f,r}}{\delta_f}$ at the two axles.

shows respectively the transfer function of the normalized load transfers ($\frac{R_{f,r}}{\delta_f}$) and the input currents $\frac{u_{f,r}}{\delta_f}$ at the two axles, as well as the inverse of the weighting functions ($\frac{1}{W_{zRf}}, \frac{1}{W_{zRr}}, \frac{1}{W_{zuf}}, \frac{1}{W_{zur}}$). As shown in Figures $4a,b$ and Table 4, the LPV active anti-roll bar system allows to reduce the normalized load transfers (at the two axles) compared with the passive anti-roll bar case in the frequency range up to more than $4 rad/s$, which represents the limited bandwidth of the driver [9].

Figures $4c,d$ show the transfer function gains of the input currents at the front ($\frac{u_f}{\delta_f}$) and rear axles ($\frac{u_r}{\delta_f}$), respectively. When the forward velocity increases, the controller input currents ($u_{f,r}$) also increase. This indicates that the active anti-roll bar system requires more input current (i.e. energy) at higher forward velocity. Nonetheless, it remains in the allowed bound, which prevents from the actuator saturation.

Table 4: Reduction of the magnitude of Transfer Functions (TF) compared with the passive case at 40 km/h and 130 km/h.

TF	$v = 40 km/h$	$v = 130 km/h$
$\frac{R_f}{\delta_f}$	11 dB [0, 4 rad/s]	18 dB [0, 5 rad/s]
$\frac{R_r}{\delta_f}$	14 dB [0, 10 rad/s]	16 dB [0, 10 rad/s]

5.1.2. *The 2nd case:* $\rho_{2,3} = [0,1]$ *(5 grid points)*

We consider the varying parameter $\rho_1 = v = 70\ km/h$, while the varying parameters $\rho_{2,3} = [0,1]$ with 5 grid points for each parameter. Figure 5 shows the transfer function magnitude of the normalized load transfers at the two axles $\frac{R_{f,r}}{\delta_f}$ when the varying parameters $\rho_{2,3}$ are at the lower and upper bounds ($\rho_2 = 0$, $\rho_2 = 1$ and $\rho_3 = 0$, $\rho_3 = 1$).

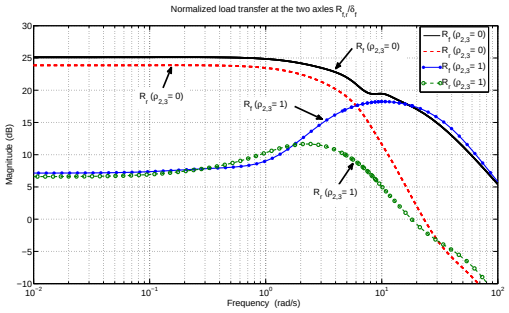

Figure 5: Transfer function magnitude of the normalized load transfers at the two axles $\frac{R_{f,r}}{\delta_f}$.

As shown in Figure 5, when the value of $\rho_{2,3}$ increase, the normalized load transfers at the two axles decrease in the frequency range up to more than $4\ rad/s$. And the reduction is about $19dB$ between $\rho_{2,3} = 0$ and $\rho_{2,3} = 1$. The results above, indicate that the proposed H_∞/LPV controller (with the parameter dependent weighting functions, including the normalized load transfers at the two axles) provides for performance adaptation to the rollover risk for heavy vehicles.

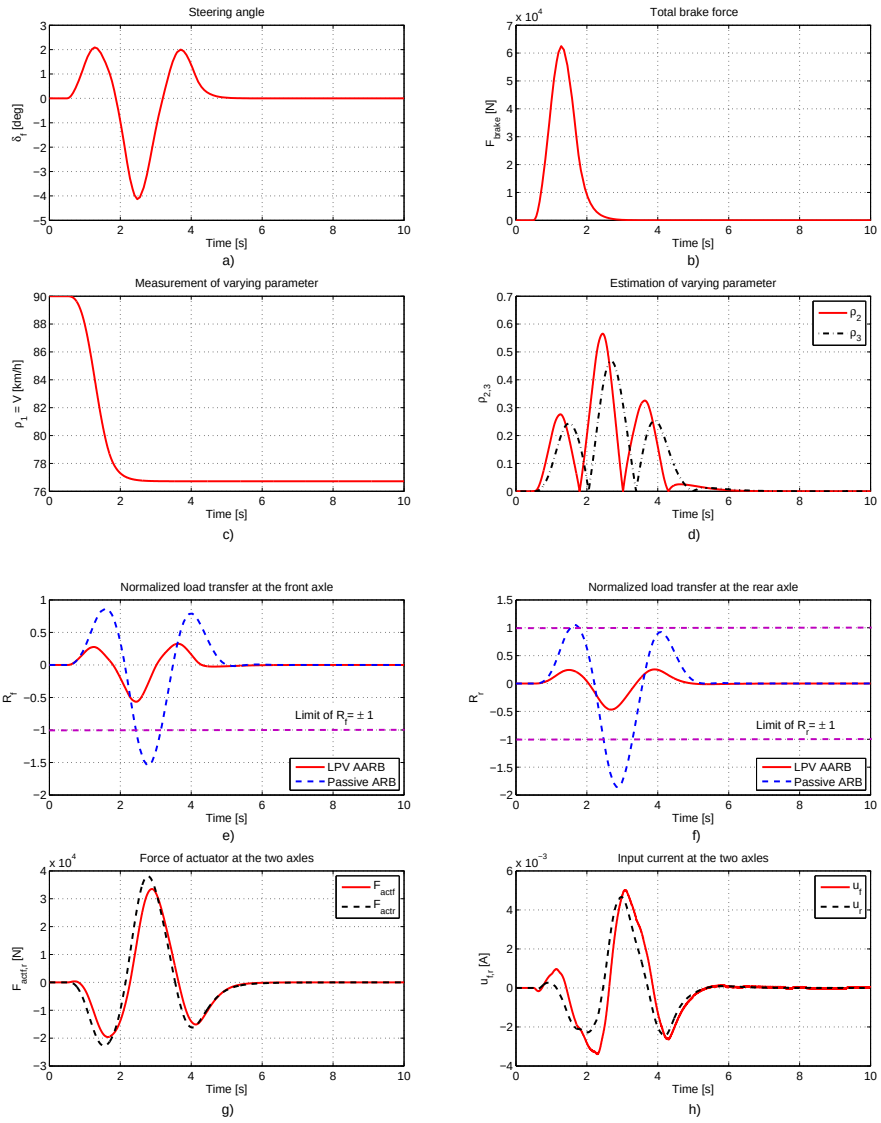

Figure 6: Time responses of the heavy vehicle in the double lane change manoeuver to avoid obstacle.

5.2. *Analysis in the time domain*

In this section, some simulation results in the time domain are shown for two different situations: the passive anti-roll bar and the LPV active anti-roll bar of the integrated model. The vehicle manoeuvre is a double lane change, which is a typical case to evaluate for the obstacle avoidance in an emergency. The manoeuvre has a 2.5 m path deviation over 100 m. The steering angle δ_f is shown in Figure 6a.

To validate the proposed H_∞/LPV controller strategy for the active anti-roll bar system with three varying parameters $\rho_1 = v$, $\rho_2 = |R_f|$, $\rho_3 = |R_r|$, the following scenario is used:

- The initial forward velocity is 90 km/h, the vehicle runs on the dry road ($\mu = 1$). The total rolling resistance and aerodynamic resistance forces are ignored.
- When the obstacle is detected, the driver reduces the throttle and brakes to reduce the forward velocity of the vehicle. The total brake force increases from 0.5s to 1.5s and then the driver takes off the brake pedal, as shown in Figure 6b.

The differential equation for the forward velocity in case of the braking situation is determined as [24]:

$$m\dot{v} = -\sum_{i=1}^{4} F_{bi} \tag{20}$$

where F_{bi} is the brake force at the each wheel. Due to the brake force, the forward velocity reduces from 90 km/h to 76.5 km/h, as in Figure 6c.

Figures 6c,d show the variation of varying parameters $\rho = [\rho_1, \rho_2, \rho_3]$. Figures 6$e,f$ show the normalized load transfers at the two axles. We can see that in the case of the passive anti-roll bar system, the rollover does occur indeed at the two axles, but in the case of the H_∞/LPV active anti-roll bar control, the maximum absolute value of the normalized load transfers at the two axles are respectively 0.55 and 0.46. This indicates that the H_∞/LPV active anti-roll bar control improves well the roll stability of heavy vehicles compared with the passive anti-roll bar case. The force of the actuators as well as the input current at the two axles are shown in Figure 6g,h.

The simulation results both in frequency and time domains have proved the effectiveness of the H_∞/LPV active anti-roll bar controller synthesis, which considered the three varying parameters: the forward velocity and the normalized load transfers at the two axles, compared with the passive anti-roll bar case.

6. Validation of the H_∞/LPV active anti-roll bar control by using the TruckSim® simulation software

TruckSim®[1] is a vehicle dynamics modelling software developed by Mechanical Simulation. It delivers accurately, detailed, and efficient methods for simulating the performance of multi-axle commercial vehicles such as 4×2 tractors, 6×4 tractors as well as box trucks, buses and trailers. From TruckSim® software, we can build vehicle models by defining many vehicle parameters which affect the dynamic behaviour of the model.

To survey the proposed H_∞/LPV controller for the active anti-roll bar system by using the nonlinear vehicle model in TruckSim® software, the authors use the co-simulation between Matlab®/Simulink® and TruckSim® software. The diagram of the co-simulation is shown in Figure 7. The nonlinear vehicle model is determined from TruckSim® software, based on using the block S-function of Simulink. Meanwhile, the controller and the actuators are built directly in the Matlab®/Simulink® environment.

[1] Mechanical Simulation Corporation, http://carsim.com/products/trucksim/

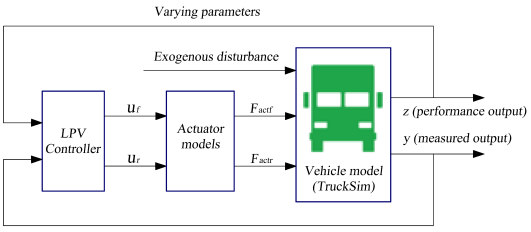

Figure 7: Diagram of TruckSim®-Simulink® Co-Simulation.

In the following validations, the authors tested the proposed H_∞/LPV controller for the active anti-roll bar system with two different types of vehicle: the tour bus and the LCF (Low Cab Forward) truck using the solid suspension system, both fully loaded. The engine is mounted at the rear of the vehicle for the tour bus and at the front for the LCF truck. To evaluate the rollover of vehicles, we consider the tyre force (F_z) in the Z direction at the each wheel (rollover occurs when $F_z = 0$). The authors note that the steering angle in the following section is the angle of the steering wheel, which is directly controlled by the driver. In the co-simulation between Matlab®/Simulink® and TruckSim®, there are two solutions for the steering angle:

Figure 8: Tour bus 2 axles (4 × 2) [38].

- First solution: the steering angle is made in Simulink® and entered to TruckSim® through the S-function. With this solution, the trajectories of vehicle in the cases of the passive anti-roll bar and of the active anti-roll bar are often different, by the effect of the wheels lift off the road.
- Second solution: the steering angle is automatically changed to adapt with the vehicle trajectory. Here, the vehicle trajectories in the case of the passive anti-roll bar and of the active anti-roll bar will follow the target path, which fits the driver's wishes.

In the following validations, the second solution is used to define the steering angle.

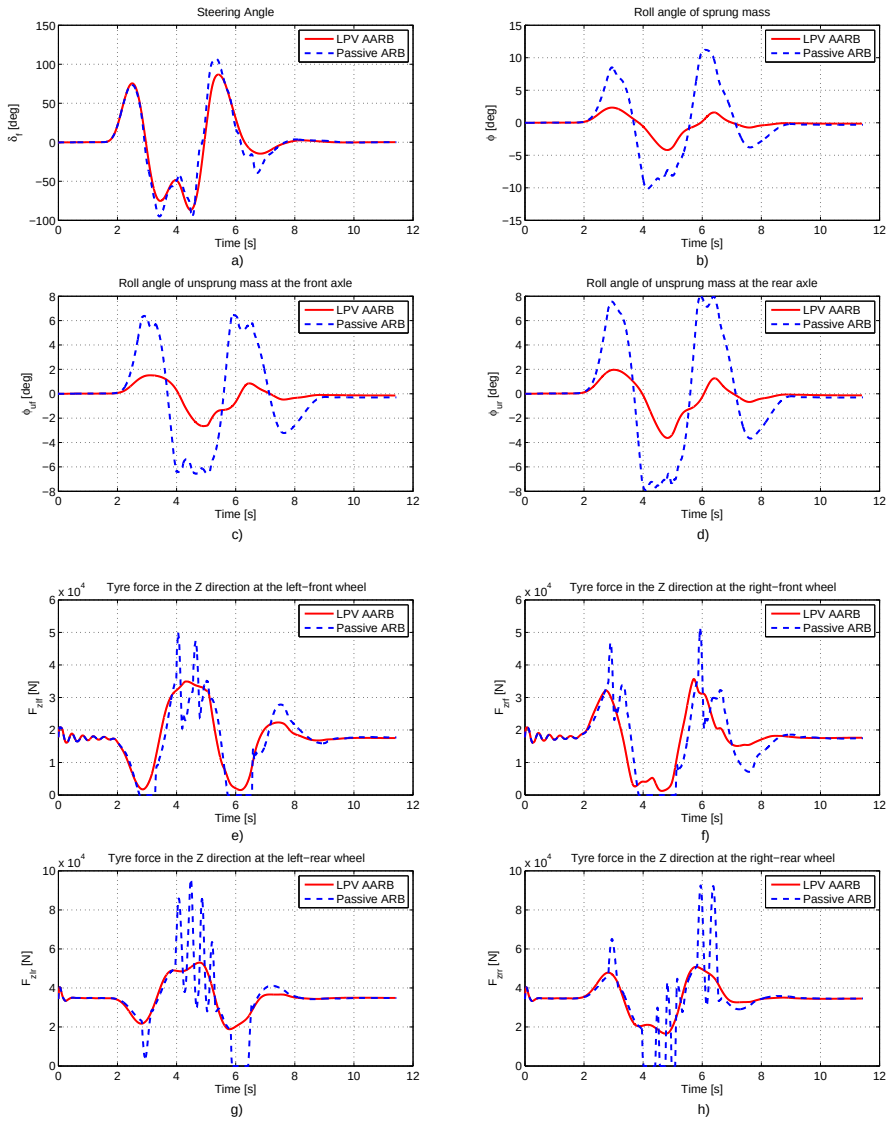

Figure 9: Time responses of the tour bus in the double lane change manoeuver.

6.1. Validation with the tour bus

A commercial passenger bus is probably one of the most popular people carrying vehicles in the world. Typically they are two axled vehicles (bus 2A) with a capacity of 45 passengers, as shown in Figure 8. In this validation, the total vehicle mass of the tour bus is 10620 kg, the double lane change is used to evaluate the roll stability of the tour bus when it runs at 100 km/h, as shown in Figure 9a. This represents the situation when the driver wishes to overtake another vehicle. Figure 9 shows the time responses of the tour bus in the double lane change manoeuver with the continued line for the H_∞/LPV active anti-roll bar and the dash line for the passive anti-roll bar.

Figures 9b,c,d show the time response of the roll angle of the sprung mass and the roll angle of the unsprung masses at the two axles, respectively. We can see that in the case of the H_∞/LPV active anti-roll bar controller, the roll angle of sprung and unsprung masses are significantly reduced compared to the passive anti-roll bar case (the reduction of the roll angle is about 6 deg for the sprung mass, 3 deg for the unsprung mass at the

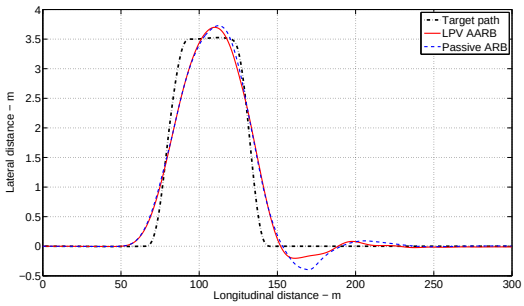

Figure 10: Trajectory of the tour bus in the double lane change manoeuver.

front and 4 deg for the unsprung mass at the rear axle). Figures $9e, f, g, h$ show the time response of the tyre forces in the Z direction of all the wheels. We can see that in the case of the H_∞/LPV active anti-roll bar controller, all the tyre forces remain positive, it means that there is no wheel lift off the road. But in the case of the passive anti-roll bar, the left-front wheel lifts off at $2.6s \div 3.4s$ and $5.7s \div 6.5s$, the right-front wheel at $3.8s \div 5.3s$, the left-rear wheel at $5.8s \div 6.5s$, the right-rear wheel at $4s \div 5.5s$. These results show that the H_∞/LPV active anti-roll bar controller drastically improves the roll stability in the case of the tour bus fully loaded.

Figure 10 shows the trajectory of the tour bus in the double lane change maneuver. We would like that, in ideal conditions, the center of the vehicle mass follows the target path. But in fact, the trajectory of the center of the vehicle mass of the real vehicle can not satisfy that (due to the impact of the suspension system, the wheelbase and the wheels lift off from the road, etc). The trajectory of the vehicle in both cases of the H_∞/LPV active anti-roll bar and the passive anti-roll bar can only stick with the ideal target path as in Figure 10. Figure $9a$ shows the steering wheel angle controlled by the driver with the amplitude about 100 deg. To ensure the trajectory of the vehicle as in Figure 10, the driver generates the steering wheel angle difference between the H_∞/LPV active anti-roll bar case and the passive anti-roll bar case. We can easily see that the steering wheel angle in the case of the H_∞/LPV active anti-roll bar is smoother than in the case of the passive anti-roll bar. Thus, in the H_∞/LPV active anti-roll bar case, the driver is less tired than in the passive anti-roll bar case.

Figure 11: LCF truck 2 axles (4×2) [39].

6.2. *Validation with the LCF truck*

In this validation, the total vehicle mass of the LCF truck is 12549 kg, a sine wave steering manoeuver is used to evaluate the roll stability of the LCF truck when it runs at 80 km/h, as shown in Figure $12a$.

Figure 12 shows the time response of the LCF truck. From figure $12a$, the steering wheel angle δ_f is the sine wave with the amplitude of 90 deg and the repeating cycle time is $4s$. In this validation, the driver applies the same steering wheel angles for both the H_∞/LPV active anti-roll bar case and the passive anti-roll bar case.

Figures $12b, c, d$ show that in the case of the H_∞/LPV active anti-roll bar control, the roll angle of sprung and unsprung masses are significantly reduced compared to the case of the passive anti-roll bar, with the reduction of 10 deg for the roll angle of sprung and of 8 deg for the roll angle of the unsprung mass at the front axle, and 3 deg for the roll angle of the unsprung mass at the rear axle.

Figures $12e, f, g, h$ show the time response of the tyre forces in the Z direction of all the wheels. We can see that in the case of the H_∞/LPV active anti-roll bar controller, all the tyre forces remain positive, which means that there is no wheel lift off the road. But in the case of the passive anti-roll bar, all the wheels at the two axles lift off. These results show that the LPV active anti-roll bar control improves the roll stability in the case of the fully loaded LCF truck.

Figure 13 shows the trajectory of the LCF truck. We can see that even the forward velocity is held constant at 80 km/h but the LCF truck travels to point A in the case of the passive anti-roll bar, and to point B in the case of the H_∞/LPV active anti-roll bar. Since the wheels lift off the road in the case of the passive anti-roll bar, some performance characteristics of the vehicle are lost.

The simulation results for both the tour bus and LCF truck show a chaotic behavioural difference: the wheels at the front axle lift off the road before the wheels at

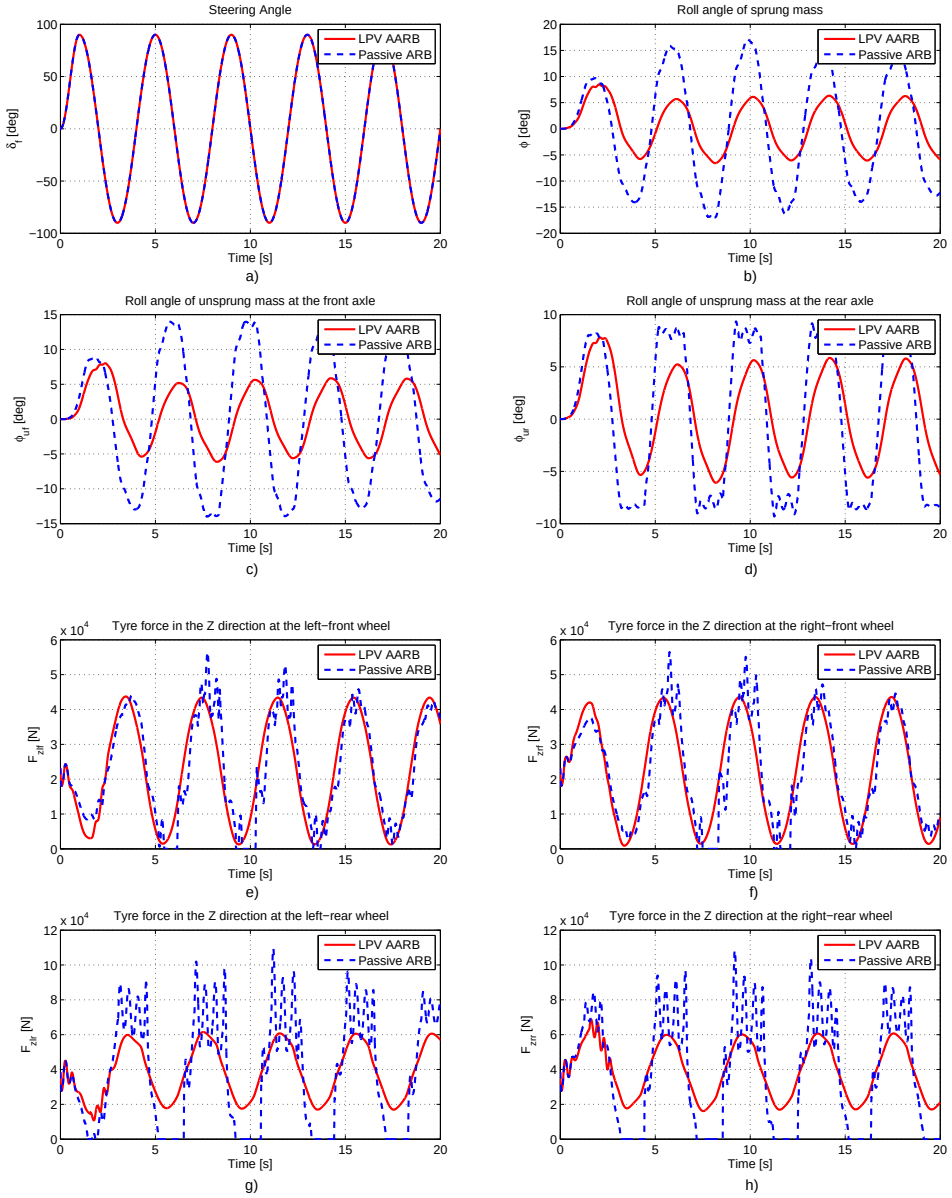

Figure 12: Time responses of the truck in the sine wave steering manoeuver.

the rear axle for the tour bus (see Figure 9g,h). And for the LCF truck, it is the opposite (see Figure 12g,h). So the rollover risk of heavy vehicles is not the same for all the types heavy vehicles. Therefore, the proposed H_∞/LPV controller with the parameter dependent weighting functions including the normalized load transfers at the two axles allows adapting the performance against the rollover risk for all types of heavy vehicles.

7. Conclusion

In this paper, the authors considered the nonlinear model of a single unit heavy vehicle as an LPV model, with the forward velocity as a scheduling parameter. The H_∞/LPV active anti-roll bar controller is synthesized by using the grid-based LPV approach through LPVTools^{TM}. Three varying parameters are considered to schedule the H_∞/LPV controller: the forward veloc-

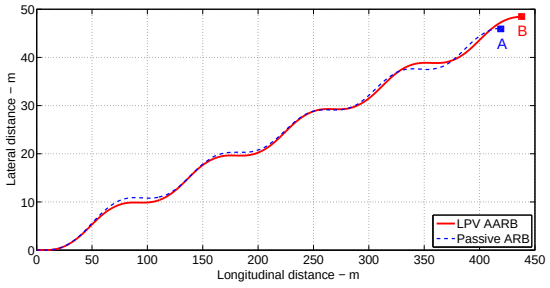

Figure 13: Trajectory of the truck in the sine wave manoeuver.

ity and the normalized load transfers at the two axles. The H_∞/LPV design is performed using parameter dependant weighting functions which allow adapting the performance to the risk of rollover in heavy vehicles.

The simulation results in the frequency and time domains as well as the validation by using the TruckSim® software show that the H_∞/LPV active anti-roll bar controller drastically improves the roll stability of the single unit heavy vehicle compared with the passive anti-roll bar.

In the future, the effect of the oil passing through the electronic servo-valve on the closed-loop system by using a LPV approach for fault tolerant control design will be also an interesting area for further research.

References

[1] A. Mige, D. Cebon, Design and implementation of an active roll control system for heavy vehicles, in: 6^{th} International Symposium on Advanced Vehicle Control, AVEC 2002, Hiroshima, Japan, 2002.

[2] H. Imine, L. M. Fridman, T. Madani, Steering control for rollover avoidance of heavy vehicles, IEEE Transactions on Vehicular Technology 61 (8) (2012) 3499–3509.

[3] D. Odenthal, T. Bunte, J. Ackermann, Nonlinear steering and braking control for vehicle rollover avoidance, in: European Control Conference, Germany, 1999.

[4] D. J. Cole, Fundamental issues in suspension design for heavy road vehicles, Vehicle System Dynamics: International Journal of Vehicle Mechanics and Mobility 35 (4-5) (2001) 319–360.

[5] M. Ieluzzi, P. Turco, M. Montiglio, Development of a heavy truck semi-active suspension control, Control Engineering Practice 14 (3) (2006) 305–312.

[6] D. J. M. Sampson, Active roll control of articulated heavy vehicles, Ph.D. thesis, University of Cambridge, UK (2000).

[7] P. Gaspar, J. Bokor, I. Szaszi, The design of a combined control structure to prevent the rollover of heavy vehicles, European Journal of Control 10 (2) (2004) 148–162.

[8] D. Sampson, D. Cebon, Active roll control of single unit heavy road vehicles, Vehicle System Dynamics: International Journal of Vehicle Mechanics and Mobility 40 (4) (2003) 229–270.

[9] D. Sampson, D. Cebon, Achievable roll stability of heavy road vehicles, in: Proceedings of the Institution of Mechanical Engineers, Part D: Journal of Automobile Engineering, Vol. 217, United Kingdom, 2003, pp. 269–287.

[10] J. Mohammadpour, C. Scherer, Control of Linear Parameter Varying Systems with Applications, Springer, 2012.

[11] O. Sename, P. Gaspar, J. Bokor, Robust Control and Linear Parameter Varying Approaches: Application to Vehicle Dynamics, Springer, 2013.

[12] D. Sampson, D. Cebon, An investigation of roll control system design for articulated heavy vehicles, in: 4th International symposium on Advanced Vehicle Control, AVEC1998, Nagoya, Japan, 1998.

[13] A. Mige, D. Cebon, Optimal roll control of an articulated vehicle: theory and model validation, Vehicle System Dynamics: International Journal of Vehicle Mechanics and Mobility 43 (12) (2005) 867–884.

[14] P. Gaspar, J. Bokor, I. Szaszi, Reconfigurable control structure to prevent the rollover of heavy vehicles, Control Engineering Practice 13 (6) (2005) 699–711.

[15] P. Gaspar, Z. Szabo, J. Bokor, Prediction based combined control to prevent the rollover of heavy vehicles, in: Proceedings of the 13th Mediterranean Conference on Control and Automation, Limassol, Cyprus, 2005.

[16] V.-T. Vu, O. Sename, L. Dugard, P. Gaspar, H_∞ active anti-roll bar control to prevent rollover of heavy vehicles: a robustness analysis, in: IFAC Symposium on System Structure and Control - 6^{th} SSSC 2016, Istanbul, Turkey, 2016.

[17] H. Yu, L. Guvenc, U. Ozguner, Heavy duty vehicle rollover detection and active roll control, Vehicle System Dynamics: International Journal of Vehicle Mechanics and Mobility 46 (6) (2008) 451–470.

[18] V.-T. Vu, O. Sename, L. Dugard, P. Gaspar, Active anti-roll bar control using electronic servo-valve hydraulic damper on single unit heavy vehicle, in: IFAC Symposium on Advances in Automotive Control - 8^{th} AAC 2016, Norrköping, Sweden, 2016.

[19] V.-T. Vu, O. Sename, L. Dugard, P. Gaspar, Enhancing roll stability of heavy vehicle by lqr active anti-roll bar control using electronic servo-valve hydraulic actuators, Vehicle System Dynamics: International Journal of Vehicle Mechanics and Mobility 55 (9) (2017) 1405–1429.

[20] F. Wu, Control of linear parameter varying systems, Ph.D. thesis, University of California at Berkeley, USA (1995).

[21] H. Merritt, Hydraulic control systems, John Wiley & Sons, 1967.

[22] A. B. Rafa, A. F. Yahya, E. J. T. Rawand, A study on the effects of servo-valve lap on the performance of a closed - loop electrohydraulic position control system, Al-Rafidain Engineering 17 (5) (2009) 1–14.

[23] H. Hsun-Hsuan, K. Rama, A. G. Dennis, Active roll control for rollover prevention of heavy articulated vehicles with multiple-rollover-index minimisation, Vehicle System Dynamics: International Journal of Vehicle Mechanics and Mobility 50 (3) (2012) 471–493.

[24] P. Gaspar, Z. Szabo, J. Bokor, The design of an integrated control system in heavy vehicles based on an LPV method, in: Proceedings of the 44th IEEE Conference on Decision and Control, and the European Control Conference, Seville, Spain, 2005.

[25] F. Wu, A generalized LPV system analysis and control synthesis framework, International Journal of Control 74 (7) (2001) 745–759.

[26] F. Wu, X. H. Yang, A. Packard, G. Becker, Induced L2-norm control for LPV systems with bounded parameter variation rates, International Journal of Robust and Nonlinear Control 6 (9-10) (1996) 983–998.

[27] C. Hoffmann, H. Werner, Complexity of implementation and synthesis in linear parameter-varying control, in: IFAC World

Congress - 19^{th} IFAC WC 2014, Cape Town, South Africa, 2014.

[28] A. Packard, Gain scheduling via linear fractional transformations, Systems and Control Letters 22 (2) (1994) 79–92.

[29] P. Apkarian, P. Gahinet, A convex characterization of gain-scheduled H_∞ controllers, IEEE Transactions on Automatic Control 40 (5) (1995) 853–864.

[30] C. Scherer, P. Gahinet, M. Chilali, Multiobjective output-feedback control via LMI optimization, IEEE Transactions on Automatic Control 42 (7) (1997) 896–911.

[31] G. Becker, Quadratic stability and performance of linear parameter dependent systems, Ph.D. thesis, University of California at Berkeley, USA (1993).

[32] P. Gahinet, P. Apkarian, M. Chilali, Affine parameter-dependent lyapunov functions and real parametric uncertainty, IEEE Transactions on Automatic Control 41 (3) (1996) 436–442.

[33] A. Hjartarson, P. Seiler, G. J. Balas, LPV aeroservoelastic control using the LPVtools toolbox, in: AIAA Atmospheric Flight Mechanics, United States, 2013.

[34] W. Yi, S. Hongjun, P. Kapil, B. M. J, S. P. M, Model order reduction of aeroservoelastic model of flexible aircraft, in: 57^{th} Structures Structural Dynamics and Materials Conference, California, United States, 2016.

[35] A. Marcos, G. J. Balas, Development of linear-parameter-varying models for aircraft, Journal of Guidance, Control, and Dynamics 27 (2) (2004) 218–228.

[36] A. Hjartarson, P. Seiler, A. Packard, LPVtools: A toolbox for modeling, analysis, and synthesis of parameter varying control systems, in: First IFAC Workshop on Linear Parameter Varying Systems, France, 2015.

[37] S. Hecker, Generating structured LPV-models with maximized validity region, in: IFAC World Congress - 19^{th} IFAC WC 2014, Cape Town, South Africa, 2014.

[38] Tour-bus, `https://www.grenoble-congres.com/fr/catalogue/activite/navette-grenoble-aeroport-geneve-gva-632985/`.

[39] LCF-Truck, `http://jingletruck.com/2006-ford-lcf-16ft-43932`.